pH-Dependent Interaction of Fumonisin B₁ with Cholesterol: Physicochemical and Molecular Modeling Studies at the Air–Water Interface

Radhia Mahfoud,[†] Marc Maresca,[†] Maurice Santelli,[‡] Annie Pfohl-Leszkowicz,[§] Antoine Puigserver,[†] and Jacques Fantini*,[†]

Institut Méditerranéen de Recherche en Nutrition, UMR-INRA 1111, and Laboratoire de Synthèse Organique, Faculté des Sciences de St-Jérôme, 13397 Marseille Cedex 20, France; and ENSAT, Laboratoire de Toxicologie et Sécurité Alimentaire, 31326 Auzeville-Tolosane, France

Langmuir film balance technology was used to study the interaction between the mycotoxin fumonisin B₁ (FB₁) and cholesterol. FB₁ was added in the aqueous subphase underneath a monomolecular film of cholesterol, and the interaction was measured as an increase in the surface pressure of the film. Above pH 9, a strong inhibition of the reaction was observed. Similar results were obtained with the bile salt sodium taurocholate. The FB₁−cholesterol complex was reinforced by NaCl but was destabilized by NaF, a salt known to break hydrogen bonds. These data suggest that the molecular association between FB₁ and cholesterol involves both hydrophobic interactions and a hydrogen bond between the NH₃⁺ group of FB₁ and the OH group of cholesterol. Molecular mechanics simulations of the FB₁−cholesterol complex were consistent with this hypothesis. These data may shed some light on the mechanisms involved in the intestinal absorption of FB₁ and its biliary excretion.

KEYWORDS: Fumonisin B₁; monomolecular film; interface; cholesterol; sodium taurocholate

INTRODUCTION

The fumonisins are a group of recently characterized mycotoxins produced by *Fusarium* molds, in particular *F. verticillioides* and *F. proliferatum*, which contaminate maize and various cereals around the world (*1, 2*). Fumonisin B₁ (FB₁) is always the most abundant fumonisin in naturally contaminated foods and feeds (*3*). FB₁ presents structural similarities with sphingosine and sphinganine and interferes with ceramide synthase (EC 2.3.1.24), leading to the accumulation of sphingoid bases in exposed cells. This affects several key biological processes such as cell proliferation and DNA replication (*4−6*). In addition to this principal effect, FB₁ induces lipid peroxidation (*6, 7*) and mitogen-activated protein kinase (MAPK) activity (*8*). In vivo, FB₁ is responsible for a wide range of biological effects including leukoencephalomalacia in horses (*9*), pulmonary edema in pigs (*10*), and nephrotoxicity and liver cancers in rats (*11, 12*). In humans, FB₁ has been associated with a high incidence of esophageal cancer in Transkei (southern Africa) and in certain areas of China (*13*).

The mechanisms associated with the intestinal absorption of FB₁ are mostly unknown. In laying hens, the systemic absorption of orally given FB₁ appeared to be very poor (<1%) (*14*). Similar data were obtained in cows (*15*). In pigs, the bioavailability of FB₁ following intragastric administration was estimated to be 3−6% (*16*). The marked alteration of FB₁ elimination profiles in bile-interrupted pigs suggested that the mycotoxin underwent enterohepatic circulation. The bioavailability of ¹⁴C-labeled FB₁ appeared to be slightly higher in male Sprague−Dawley rats (*17*). In this case, up to 35% of the radiolabel were eliminated in the feces, indicating that the mycotoxin or its metabolites undergo biliary excretion. Moreover, the same authors reported that up to 50% of FB₁ injected intravenously in a bile duct cannulated rat was excreted unchanged in bile. These data raise the interesting possibility that the mycotoxin could interact with bile components such as cholesterol and bile salts. The structural similarity between FB₁ and sphingoid bases and the previously reported interaction between cholesterol and sphingolipids (*18, 19*) support this hypothesis.

The aim of the present study was to investigate the potential interactions between FB₁ and cholesterol (or FB₁ and sodium taurocholate), using Langmuir film balance technology. In these experiments, a monomolecular film of lipid (cholesterol or sodium taurocholate) was prepared at the air−water interface and FB₁ was added in the aqueous subphase. The interaction of the mycotoxin with the lipid film was measured as an increase in the surface pression of the film. This technique is one of the most sensitive for studying lipid−ligand interactions (*20*). The microtensiometer used in the present study can measure the surface tension of liquid volumes of 500−800 μL. Correspondingly, the amount of FB₁ used in binding experiments was 12

* Corresponding author (telephone +33 491-288-761; fax +33 491-288-440; e-mail j.fantini@caramail.com).
† Institut Méditerranéen de Recherche en Nutrition.
‡ Laboratoire de Synthèse Organique.
§ ENSAT, Laboratoire de Toxicologie et Sécurité Alimentaire.

328 *J. Agric. Food Chem.,* Vol. 50, No. 2, 2002

Mahfoud et al.

μg (i.e., 20 μM). Molecular mechanics simulations were conducted to characterize the complex between FB$_1$ and cholesterol. This modeling technique was validated by its ability to predict the more stable conformation of FB$_1$ in water in comparison with previous modeling studies (*21*).

MATERIALS AND METHODS

Materials. The chemicals used in this study, including FB$_1$, cholesterol, and sodium taurocholate of the highest purity available, were purchased from Sigma.

Surface Pressure Measurements. The surface pressure was measured with a fully automated microtensiometer (μTrough SX, Kibron Inc., Helsinki, Finland). The apparatus allowed the recording of pressure$-$area compression isotherms and the kinetics of interaction of a ligand with the monomolecular film, using a set of specially designed Teflon troughs. All experiments were carried out in a controlled atmosphere at 20 $\pm$ 1 °C. Monomolecular films of the indicated lipids were spread on pure water subphases (volume of 800 μL) from hexane/chloroform/ethanol (11:5:4, v/v/v) as described previously (*22*). After spreading of the film, 5 min was allowed for solvent evaporation. To measure the interaction of FB$_1$ with lipid monolayers, the ligand was injected in the subphase with a 10 μL Hamilton syringe, and pressure increases produced were recorded for the indicated time. In some experiments, the subphase was prepared at various pH values. For experiments with NaCl and NaF, the subphase was prepared with the indicated concentration of salt before the addition of FB$_1$. The data were analyzed with the Filmware 2.3 program (Kibron Inc.). The accuracy of the system under our experimental conditions was ±0.25 mN/m for surface pressure.

Curve Fitting. Experimental data were analyzed with the Origin program, version 3.5 (Microcal software). The Boltzman (x, A_1, A_2, x_0, dx) function producing a sigmoidal curve was used according to the equation

$$(A_1 - A_2)/[1 + \exp((x - x_0)\, \mathrm{d}x)] + A_2$$

with parameters of x_0 (center, i.e., x at y_{50}), dx (width), A_1 (*Y* initial), and A_2 (*Y* final).

Molecular Modeling. Molecular mechanics simulations were performed with the Hyperchem 5 program (ChemCAD, Obernay, France). A box with periodic boundaries was created to allow application of image conditions, and the molecules (i.e., FB$_1$ alone or FB$_1$ with two cholesterol molecules) were placed in the box. For modeling the FB$_1-$cholesterol complex, 331 water molecules were added to the box (27 $\times$ 22 $\times$ 31 Å), and energy minimization was carried out with the Polak$-$Ribiere algorithm. The efficiency of the minimization was judged by both the time needed to evaluate the target function and the number of adjustments (iterations) needed to converge to the minimum.

RESULTS

Interaction of FB$_1$ with Cholesterol. Cholesterol (2 μg) was spread at the air$-$water interface at an initial surface pressure of 10 mN/m. Various concentrations of FB$_1$ were then added in the aqueous subphase. The interaction of the mycotoxin with the cholesterol monolayer was studied by surface pressure measurements. As shown in Figure 1A, FB$_1$ induced a dose-dependent increase of surface pressure ($\Delta\pi$), with a half-maximal effect obtained with a concentration of FB$_1$ of 7.5 μM. The maximal surface pressure increase ($\Delta\pi_{max}$ = 15 mN/m) was obtained with 20 μM FB$_1$. At all concentrations of FB$_1$, the equilibrium was reached within 1 min upon addition of the toxin.

To assess the specificity of FB$_1-$cholesterol interaction, monomolecular films of cholesterol were prepared at various initial pressures (π_i) and the maximal surface pressure increase induced by FB$_1$ on these films was determined after equilibrium had been reached. As shown in Figure 1B, the compressibility
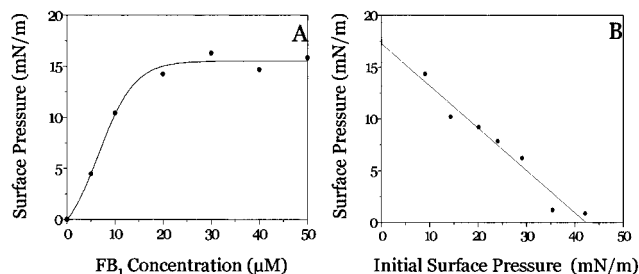

Figure 1. Specific interaction between FB$_1$ and cholesterol: (A) dose-dependent interaction between FB$_1$ and a monomolecular film of cholesterol prepared at an initial pressure (π_i) of 10 mN/m (increases in the surface pressure induced by the indicated concentrations of FB$_1$ added in the aqueous subphase were determined); (B) specificity of interaction between FB$_1$ and cholesterol films prepared at various π_i values [after FB$_1$ was added at a concentration of 20 μM in the aqueous subphase, the maximal surface pressure increase ($\Delta\pi_{max}$) was measured].

of the monomolecular film was gradually decreased as the initial pressure of the monolayer increased. The influence of the initial surface pressure on the compressibility of the cholesterol monolayer demonstrates the high specificity of the interaction as previously established for several other lipids and ligands (*23*). The critical pressure of insertion (i.e., the theoretical value of π_i extrapolated for $\Delta\pi_{max}$ = 0 mN/m) was 42 mN/m.

Effect of Salts and pH on FB$_1$—Cholesterol Interaction. With the aim to identify the chemical groups involved in the interaction between FB$_1$ and cholesterol, we studied the reaction in the presence of various concentrations of salts and at different pH values. Two types of salts were used: NaCl, which destabilizes ionic bonds and reinforces hydrophobic interactions, and NaF, which interferes with the establishment of hydrogen bonds. In a first set experiments, monolayers of cholesterol (π_i = 10 mN/m) were prepared on a water subphase with NaCl at concentrations ranging from 0.1 to 5 M. FB$_1$ was then added in the subphase at a concentration of 20 μM. Under these conditions, the presence of NaCl did not delay or decrease the dramatic effect of FB$_1$ on the surface pressure ($\Delta\pi_{max}$ = 15$-$17 mN/m). At high NaCl concentrations, the FB$_1$-induced surface pressure increase was even higher than the control values (19.1 and 39.5 mN/m for 1 and 5 M NaCl, respectively). In marked contrast with these data, we observed that NaF (1 M in the aqueous subphase) dramatically decreased the interaction of FB$_1$ with cholesterol ($\Delta\pi_{max}$ = 2.8 mN/m).

Similar experiments were performed with water subphases prepared at different pH values (Figure 2). The insertion of FB$_1$ (20 μM) within the monomolecular film of cholesterol was not significantly affected when the pH of the subphase was $\leq$8 (optimal pH of interaction was $\sim$6.5). However, above pH 9, the interaction of FB$_1$ with cholesterol was dramatically reduced ($\Delta\pi_{max}$ = 3 at pH 9.5). Thus, these data suggest that the binding of FB$_1$ to cholesterol involves a chemical group with a pK_a of 9$-$9.5.

Modeling Studies. Molecular mechanics simulations were performed to propose a model for the FB$_1-$cholesterol complex. This modeling technique was first validated for its ability to predict an extended conformation for FB$_1$ in water compatible with the recent model proposed by Momany and Dombrink-Kurtzman (*21*). According to these authors, the mycotoxin adopts an extended, linear conformation distinct from the previously suggested cage-like structure (*24*). Our model is consistent with the one proposed by Momany and Dombrink-Kurtzman (*21*). The molecule adopts a cross-like structure with
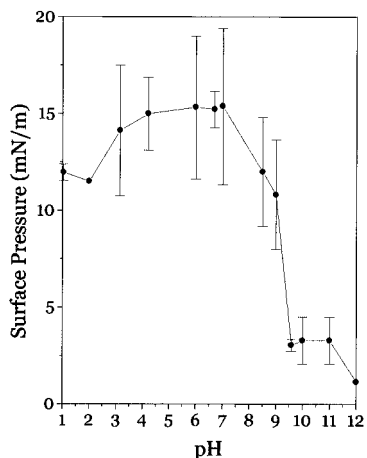
Cholesterol–Fumonisin B$_1$ Interactions

J. Agric. Food Chem., Vol. 50, No. 2, 2002 **329**

Figure 2. Effect of pH on the association between FB$_1$ and cholesterol. Monolayers of cholesterol were prepared at a π_i of 10 mN/m. FB$_1$ (20 μM) was added in the aqueous subphase at the indicated pH. The maximal surface pressure ($\Delta\pi_{max}$) induced by the mycotoxin at each pH value is shown.
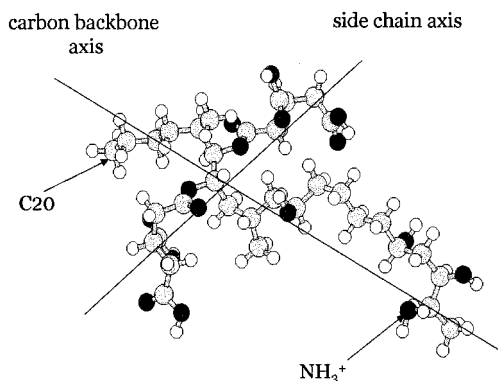

Figure 3. Conformation of FB$_1$ in solution predicted by molecular mechanics simulations.

the tricarballylic acid side chains of FB$_1$ oriented perpendicularly to the main axis of the carbon chain (Figure 3).

In the model obtained for the FB$_1$–cholesterol complex, the protonated NH$_3$$^+$ group of FB$_1$ forms a hydrogen bond with the OH group of cholesterol (Figure 4A). The tricarballylic acid side chains are localized in the aqueous environment and are kept apart from cholesterol by a structured network of water molecules (not shown). The linear carbon backbone between C16 and C20 interacts with the acyclic carbon chain of cholesterol (Figure 4A). Schematically, FB$_1$ adopts a butterfly-like structure that is spread under two adjacent cholesterol molecules (Figure 4B). FB$_1$ is attached to cholesterol by both the head (the protonated NH$_3$$^+$ group) and the tail (the linear carbon backbone between C16 and C20, and especially C18, C19, and C20), whereas the wings (the tricarballylic acid side chains) are extended through the interfacial water layer underneath the cholesterol film.

Interaction of FB$_1$ with Taurocholate. Finally, we analyzed the interaction between FB$_1$ and sodium taurocholate (Figure 5). As for cholesterol, the association between FB$_1$ and taurocholate at the air–water interface was dose-dependent, with a half-maximal effect obtained with 15 μM FB$_1$ and a maximal surface pressure increase ($\Delta\pi_{max}$ = 15.5 mN/m) obtained with 40 μM FB$_1$ (Figure 5A). The interaction decreased specifically as the initial surface pressure (π_i) increased (Figure 5B). The optimal pH for the interaction was 6.0 (data not shown).
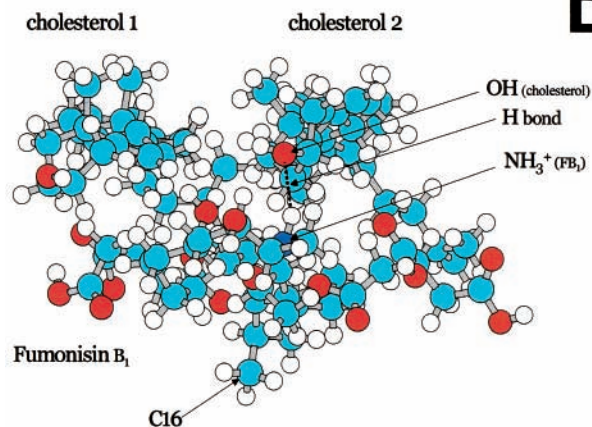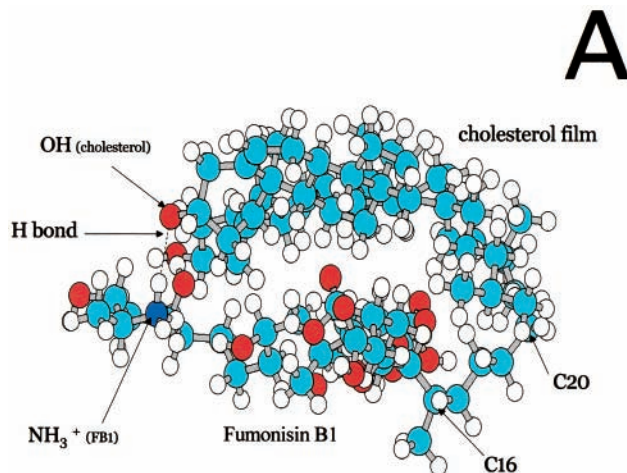

Figure 4. Molecular mechanics simulations of the FB$_1$–cholesterol complex at the air–water interface. The complex between FB$_1$ and a monomolecular film of cholesterol was visualized under two distinct orientations. For clarity, either one (A) or two (B) molecules of cholesterol and a single molecule of FB$_1$ are shown.
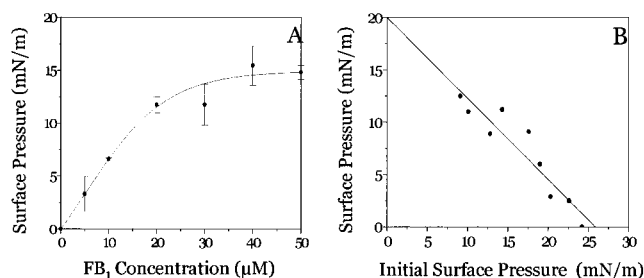

Figure 5. Specific interaction between FB$_1$ and sodium taurocholate: (A) dose-dependent interaction between FB$_1$ a monomolecular film of sodium taurocholate prepared at a π_i of 10 mN/m (increases in surface pressure induced by the indicated concentrations of FB$_1$ added in the aqueous subphase were determined); (B) specificity of interaction between FB$_1$ and monomolecular films of sodium taurocholate prepared at various π_i values [after FB$_1$ was added at a concentration of 20 μM in the aqueous subphase, the resulting surface pressure increase ($\Delta\pi_{max}$) was determined].

DISCUSSION

In this study, we show that FB$_1$ interacts with cholesterol and sodium taurocholate. This association is possible because in aqueous solution, FB$_1$ adopts a linear structure allowing a

330 *J. Agric. Food Chem.,* Vol. 50, No. 2, 2002

Mahfoud et al.

Table 1. Physicochemical Parameters of the FB_1–Cholesterol and FB_1–Sodium Taurocholate Interactions at the Air–Water Interface

parameter	cholesterol	sodium taurocholate
dose of half-maximal effect (μM)	7.5	15
dose of saturation (μM)	20	40
critical pressure of insertion (mN/m)	42	26
optimal pH	~6.5	~6.0

convenient orientation at the interface and facilitating its insertion into lipid monolayers (Figure 3). This structure was obtained by molecular mechanics simulations based on the minimization of the potential energy of the molecule as a function of its conformation. It is consistent with recent molecular dynamics simulations of FB_1 conformation (*21*). In particular, the carbon backbone of FB_1 adopts an extended conformation, and the tricarballylic acid side chains are oriented perpendicularly to the main axis of the molecule. Interestingly, the linear model is also consistent with the high water solubility of FB_1 at neutral pH. This is due to the structure of water molecules around the carboxyl groups of the tricarballylic acid side chains (*21*).

The physicochemical parameters of FB_1–cholesterol and FB_1–taurocholate interactions are summarized in Table 1. The interaction between FB_1 and these lipids was dose-dependent and saturable. As a matter of fact, the concentrations of FB_1 used in these monolayer experiments are determined by the sensitivity of the microtensiometer and may not reflect physiological conditions. Nevertheless, dietary concentrations of FB_1 that are toxic are ~20–70 μM (*25*). Therefore, the range of FB_1 concentrations used in our experiments (1–40 μM) may be physiologically relevant. Moreover, the finding of a critical pressure of insertion of 42 mN/m is indicative of a high-affinity complex between FB_1 and cholesterol. Indeed, the mean lipid density of cellular membranes corresponds to a surface pressure of 30 mN/m (*26*). At this physiological value of the surface pressure, which corresponds to a densely packed film, there is a measurable insertion of FB_1 into the cholesterol monolayer (Figure 1B). This indicates that FB_1 is able to separate two adjacent cholesterol molecules and to take place between them, inducing an increase in the surface pressure. These data demonstrate the high specificity of the binding reaction. The formation of the FB_1–cholesterol complex is pH-dependent, with a strong inhibition above pH 9 (Figure 2). In contrast, the interaction of FB_1 with cholesterol is essentially the same between pH 1 and pH 8, that is, over a range of pH values including the pK_a of the carboxylic acid groups of FB_1. Therefore, the ionization status of these groups may not play an important role in the absorption of FB_1. In contrast, it could be reasonably assumed that the pK_a for the amino group of FB_1 is around pH 9.0–9.5. Correspondingly, the strong inhibition of the interaction observed above pH 9 could reflect the requirement of the protonated amino group of FB_1. Taken together, these data suggest that (i) the carboxylic groups of FB_1 are not directly involved in the interaction with cholesterol and (ii) the amino group of FB_1 has to be protonated. Because the reaction is not inhibited by high NaCl concentrations, one can conclude that the binding of FB_1 to cholesterol is essentially of hydrophobic nature. Ionic interactions, which are sensitive to molar concentrations of NaCl, are not involved in the binding reaction. Moreover, the FB_1–cholesterol interaction was strongly inhibited by NaF, a fluor salt that destabilizes hydrogen bonds.

The molecular mechanics simulations of the FB_1–cholesterol complex allowed a molecular model that is consistent with this physicochemical study to be proposed (Figure 4). According to this model, the binding of FB_1 to cholesterol involves both hydrophobic interactions and a hydrogen bond between the NH_3^+ group of FB_1 and the OH group of cholesterol. The tricarballylic acid side chains interact with the water layer beyond the cholesterol monolayer and are not directly involved in the molecular association of FB_1 with cholesterol.

Overall, the data of the present study demonstrate that FB_1 can move from a water environment to a lipid phase containing cholesterol and/or bile salts. The ability of FB_1 to bind to cholesterol and taurocholate is consistent with previous reports suggesting that the mycotoxin undergoes enterohepatic circulation and is excreted in bile (*16, 17*). Moreover, these results may help to explain how FB_1 is taken up by the intestinal epithelium. In the intestinal lumen, dietary FB_1 could be incorporated into mixed micelles, through interactions with cholesterol and/or bile salts such as sodium taurocholate. The transfer of FB_1 into those micelles would facilitate its intestinal absorption.

LITERATURE CITED

(1) Bhat, R. V.; Shetty, P. H.; Amruth, R. P.; Sudershan, R. V. A foodborne disease outbreak due to the consumption of moldy sorghum and maize containing fumonisin mycotoxins. *J. Toxicol. Clin. Toxicol.* **1997**, *35*, 249–255.

(2) Nair, M. G. Fumonisins and human health. *Ann. Trop. Paediatr.* **1998**, *18*, S47–S52.

(3) Kuiper-Goodman, T. Mycotoxins: risk assessment and legislation. *Toxicol. Lett.* **1995**, *82/83*, 853–859.

(4) Schroeder, J. J.; Crane, H. M.; Xia, J.; Liotta, D. C.; Merrill, A. H., Jr. Disruption of sphingolipid metabolism and stimulation of DNA synthesis by fumonisin B1. A molecular mechanism for carcinogenesis associated with *Fusarium moniliforme*. *J. Biol. Chem.* **1994**, *269*, 3475–3481.

(5) Yoo, H. S.; Norred, W. P.; Wang, E.; Merrill, A. H., Jr.; Riley, R. T. Fumonisin inhibition of de novo sphingolipid biosynthesis and cytotoxicity are correlated in LLC-PK1 cells. *Toxicol. Appl. Pharmacol.* **1992**, *114*, 9–15.

(6) Abado-Becognee, K.; Mobio, T. A.; Ennamany, R.; Fleurat-Lessard, F.; Shier, W. T.; Badria, F.; Creppy, E. E. Cytotoxicity of fumonisin B1: implication of lipid peroxidation and inhibition of protein and DNA syntheses. *Arch. Toxicol.* **1998**, *72*, 233–236.

(7) Yin, J. J.; Smith, M. J.; Eppley, R. M.; Page, S. W.; Sphon, J. A. Effects of fumonisin B1 on lipid peroxidation in membranes. *Biochim. Biophys. Acta* **1998**, *1371*, 134–142.

(8) Pinelli, E.; Poux, N.; Garren, L.; Pipy, B.; Castegnaro, M.; Miller, D. J.; Pfohl-Leszkowicz, A. Activation of mitogen-activated protein kinase by fumonisin B(1) stimulates cPLA(2) phosphorylation, the arachidonic acid cascade and cAMP production. *Carcinogenesis* **1999**, *20*, 1683–1688.

(9) Duncan, K.; Kruger, S.; Zabe, N.; Kohn, B.; Prioli, R. Improved fluorometric and chromatographic methods for the quantification of fumonisins B(1), B(2) and B(3). *J. Chromatogr. A* **1998**, *815*, 41–47.

(10) Riley, R. T.; An, N. H.; Showker, J. L.; et al. Alteration of tissue and serum sphinganine-to-sphingosine ratio: An early biomarker of exposure to fumonisin-containing feeds in pigs. *Toxicol. Appl. Pharmacol.* **1993**, *118*, 105–112.

(11) Suzuki, C. A.; Hierlihy, L.; Barker, M.; Curran, I.; Mueller, R.; Bondy, G. S. The effects of fumonisin B1 on several markers of nephrotoxicity in rats. *Toxicol. Appl. Pharmacol.* **1995**, *133*, 207–214.

(12) Tolleson, W. H.; Dooley, K. L.; Sheldon, W. G.; Thurman, J. D.; Bucci, T. J.; Howard, P. C. The mycotoxin fumonisin induces apoptosis in cultured human cells and in livers and kidneys of rats. *Adv. Exp. Med. Biol.* **1996**, *392*, 237–250.

Cholesterol–Fumonisin B$_1$ Interactions

J. Agric. Food Chem., Vol. 50, No. 2, 2002 **331**

(13) Marasas, W. F.; Jaskiewicz, K.; Venter, F. S.; Van Schalkwyk, D. J. *Fusarium moniliforme* contamination of maize in oesophageal cancer areas in Transkei. *S. Afr. Med. J.* **1988**, *74*, 110−114.

(14) Vudathala, D. K.; Prelusky, D. B.; Ayroud, M.; Trenholm, H. L.; Miller, J. D. Pharmacokinetic fate and pathological effects of ^{14}C-Fumonisin B$_1$ in laying hens. *Nat. Toxins* **1994**, *2*, 81−88.

(15) Prelusky, D. B.; Savard, M. E.; Trenholm, H. L. Pilot study on the plasma pharmacokinetics of fumonisin B1 in cows following a single dose by oral gavage or intravenous administration. *Nat. Toxins* **1995**, *3*, 389−394.

(16) Prelusky, D. B.; Trenholm, H. L.; Savard, M. E. Pharmacokinetic fate of 14C-labelled fumonisin B1 in swine. *Nat. Toxins* **1994**, *2*, 73−80.

(17) Norred, W. P.; Plattner, R. D.; Chamberlain, W. J. Distribution and excretion of [14C]fumonisin B1 in male Sprague−Dawley rats. *Nat. Toxins* **1993**, *1*, 341−346.

(18) Smaby, J. M.; Brockman, H. L.; Brown, R. E. Cholesterol's interfacial interactions with sphingomyelins and phosphatidylcholines: hydrocarbon chain structure determines the magnitude of condensation. *Biochemistry* **1994**, *33*, 9135−9142.

(19) Smaby, J. M.; Momsen, M.; Kulkarni, V. S.; Brown, R. E. Cholesterol-induced interfacial area condensations of galactosylceramides and sphingomyelins with identical acyl chains. *Biochemistry* **1996**, *35*, 5696−5704.

(20) Maggio, B. The surface behavior of glycosphingolipids in biomembranes: a new frontier of molecular ecology. *Prog. Biophys. Mol. Biol.* **1994**, *62*, 55−117.

(21) Momany, F. A.; Dombrink-Kurtzman, M. A. Molecular dynamics simulations on the mycotoxin fumonisin B1. *J. Agric. Food Chem.* **2001**, *49*, 1056−1061.

(22) Fantini, J.; Hammache, D.; Pieroni, G.; Yahi, N. Role of glycosphingolipid microdomains in CD4-dependent HIV-1 fusion. *Glycoconjugate J.* **2000**, *17*, 199−204.

(23) Hammache, D.; Pieroni, G.; Yahi, N.; Delezay, O.; Koch, N.; Lafont, H.; Tamalet, C.; Fantini, J. Specific interaction of HIV-1 and HIV-2 surface envelope glycoproteins with monolayers of galactosylceramide and ganglioside GM3. *J. Biol. Chem.* **1998**, *273*, 7967−7971.

(24) Beier, R. C.; Elissalde, M. H.; Stanker, L. H. Calculated three-dimensional structures of the fumonisin B1−4 mycotoxins. *Bull. Environ. Contam. Toxicol.* **1995**, *54*, 479−487.

(25) Rheeder, J. P.; Marasas, W. F. O.; Thiel, P. G.; Sydenham, E. W.; Shephard, G. S.; Van Schalkwyk, D. J. *Fusarium moniliforme* and fumonisins in corn in relation to human esophageal cancer in Transkei. *Phytopathology* **1992**, *82*, 353−357.

(26) Quinn, P. J. Structure of biological membranes. In *The Lipid Handbook*; Gunstone, F. D., Harwood, J. L., Padley, F. B., Eds.; Chapman and Hall: New York, 1994; pp 465−485.